GNeosomes: Highly Lysosomotropic Nanoassemblies for Lysosomal Delivery

Ezequiel Wexselblatt,[†] Jeffrey D. Esko,[‡] and Yitzhak Tor*[,†]

[†]Chemistry and Biochemistry and [‡]Cellular and Molecular Medicine, University of California, San Diego, 9500 Gilman Drive, La Jolla, California 92093, United States

ABSTRACT GNeosomes, lysosomotropic lipid vesicles decorated with guanidinoneomycin, can encapsulate and facilitate the cellular internalization and lysosomal delivery of cargo ranging from small molecules to high molecular weight proteins, in a process that is exclusively dependent on cell surface glycosaminoglycans. Their cellular uptake mechanism and co-localization with lysosomes, as well as the delivery, release, and activity of internalized cargo, are quantified. GNeosomes are proposed as a universal platform for lysosomal delivery with potential as a basic research tool and a therapeutic vehicle.

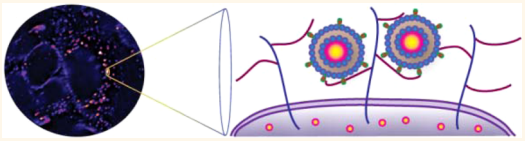

KEYWORDS: nanoassemblies · liposomes · guanidinoglycosides · cellular delivery · lysosomes

The lysosome is responsible for enzymatically breaking down and recycling large biomolecules and aged organelles.[1] While malfunctioning lysosomal enzymes have long been established as the culprit in lysosomal storage disorders (LSDs),[2] recent discoveries have suggested that defects in lysosomal enzymes (*e.g.*, glucocerebrosidase) are also linked to other chronic ailments, including neurological disorders such as Parkinson's disease and related disorders.[3−5] "Magic bullet" and targeted therapeutic delivery to the lysosome could therefore become significant in addressing such disorders. While cargo delivery to the nucleus, cytoplasm, and mitochondria has been extensively addressed,[6,7] lysosomal delivery has been mainly addressed by covalently linking cargo to carriers, only moderately enhancing lysosomotropism.[8−12] Efficient and specific delivery of intact unmodified cargo to the lysosome remains, however, a challenge despite its significant potential as a research tool and as a future therapeutic approach for lysosome-associated diseases.[13]

Over the past decade, we have developed and advanced a new family of nontoxic cellular delivery vehicles based on guanidinoglycosides.[14,15] This family of synthetic carriers is made by converting all ammonium groups on aminoglycoside antibiotics to guanidinium groups.[15] Unlike other guanidinium-rich transporters and cell-penetrating peptides (*e.g.*, Tat and oligoarginines), the cellular uptake of guanidinoglycosides occurs at nanomolar concentrations and exclusively depends on cell surface heparan sulfate (HS) proteoglycans.[16] These highly charged cell surface biopolymeric receptors, which decorate all mammalian cells, thus provide a privileged high-capacity pathway for entry into the cell.[17,18] Our studies suggest that high MW cargo, when conjugated to guanidinoglycosides, enters the cell complexed to heparan sulfate and localizes in lysosomes, where glycosaminoglycans are stored and metabolized.[19] Moreover, recent cell surface FRET analysis suggests that the multivalent nature of these conjugates is directly responsible for proteoglycan aggregation, which appears to be a pivotal step for the endocytic translocation of these carriers and their ultimate lysosomal localization.[20,21]

A key feature of the above-mentioned approach is the need to covalently link the intended cargo to the carrier, which presents the following predicaments. Conjugation of low MW bioactive agents to guanidinoglycosides might drastically alter their basic physical properties, and certain proteins might not retain their full activity when modified in this manner. Encapsulating any cargo in a molecular container such as a liposome that presents guanidinoglycosides on its periphery, thus likely retaining the cell surface HS selectivity and entry pathways, could potentially circumvent this limitation and provide a universal lysosomal

* Address correspondence to ytor@ucsd.edu.

Received for review December 25, 2014 and accepted April 1, 2015.

Published online April 01, 2015
10.1021/nn507382n

© 2015 American Chemical Society

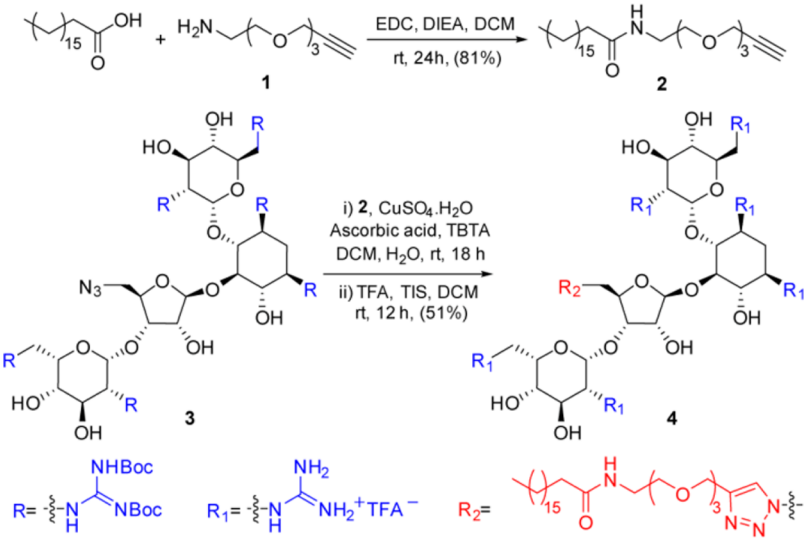

Scheme 1. Synthesis of Stearyl-GNeo, 4.

delivery vehicle for any cell-impermeable cargo. Here we disclose GNeosomes, lysosome-targeting nanocarriers. Fabricated by introducing amphiphilic guanidinylated neomycin (GNeo) into regular liposomes, these assemblies are capable of specifically delivering a wide variety of unmodified cargo into the lysosomes. We assess the delivery of cargo of diverse sizes, explore the mechanism of their uptake and cellular localization, and evaluate the cellular release and function of selected cargos.

RESULTS AND DISCUSSION

Synthesis of Stearyl-guanidinoneomycin. To present guanidinoneomycin on liposomes, stearic acid was linked to the GNeo core at the 5″ position through a triethylene glycol linker as outlined in Scheme 1. Briefly, stearic acid was coupled to the amino group of a bifunctional amino-alkyne-derivatized triethylene glycol (**1**),[22] yielding compound **2**. Subsequent 1,3-dipolar cycloaddition of **2** and **3**[21] followed by acidic deprotection of the guanidinium groups yielded Stearyl-GNeo (compound **4**, Scheme 1).[23−27]

Preparation of Lipid Vesicles. Stearyl-GNeo-decorated liposomes were prepared by rehydrating a lipid film [consisting of either POPC (1-palmitoyl-2-oleoyl-*sn*-glycero-3-phosphocholine), DOPC (1,2-dioleoyl-*sn*-glycero-3-phosphocholine), DOPC/DOPE (1,2-dioleoyl-*sn*-glycero-3-phosphoethanolamine), 85:15, or DOPC/DOPE/cholesterol, 73:11:16] with phosphate-buffered saline (PBS, pH 7.4) and Stearyl-GNeo, **4** (0.9 mol %), followed by sonication, freeze and thaw cycles, and extrusion through 100 nm polycarbonate membranes. Plain liposomes were prepared in the same manner without **4**. Dynamic light scattering analysis shows that the addition of Stearyl-GNeo results in a significant increase in zeta potential, while the average size of the liposomes and their polydispersity remain comparable (Table S1, Figure S1).[28]

Cellular Uptake. To compare and contrast the cellular uptake of plain and GNeo-containing liposomes, a water-soluble cyanine dye[29] was packaged as an emissive small molecule. Uptake was evaluated in wild-type CHO-K1 cells. The cells were incubated with liposomes at 37 °C for 1 h, harvested, and analyzed by flow cytometry. The mean fluorescence intensity (MFI) of the cells treated with decorated liposomes is remarkably higher compared to that arising from cells treated with plain liposomes (Figure 1a, Figure S3).[30] The most effective formulation consisted of DOPC/DOPE/cholesterol/GNeo, 73:11:16:0.9. These vesicles, termed GNeosomes, which showed no cytotoxicity when incubated with CHO-K1 cells for 24 h at 0.1, 0.3, and 0.5 mg mL^{-1} (Figure S4), were selected for further investigations.

Cellular uptake of GNeosomes is dose dependent and highly selective for glycosaminoglycans (GAGs), displaying extremely reduced cellular uptake in a mutant pgsA-745 cell line, which lacks heparan sulfate and chondroitin/dermatan sulfate (Figure 1b).[31] Importantly, in addition to their low overall cellular uptake, plain liposomes display no selectivity for either cell line (Figure S5). Further, to substantiate that this remarkable cellular uptake relies on the molecular nature of GNeo and not merely on augmenting the positive charge of the carrier surface, liposomes decorated with DOTAP (1,2-dioleoyl-3-trimethylammonium-propane), a cationic lipid, were evaluated. Lipid vesicles were prepared with 0.9 or 5.4 mol % DOTAP (DOTAP-M and DOTAP-N, respectively) to reflect an equimolar or equinormal ratio compared to GNeo. To evaluate the surface charge of these liposomes, their zeta potential was measured (Figure 1c inset, Table S1). The presence of DOTAP in the hydration buffer raises the zeta potential of the formed liposomes from 0.4 mV to 12 and 33 mV (plain liposomes, DOTAP-M, and DOTAP-N,

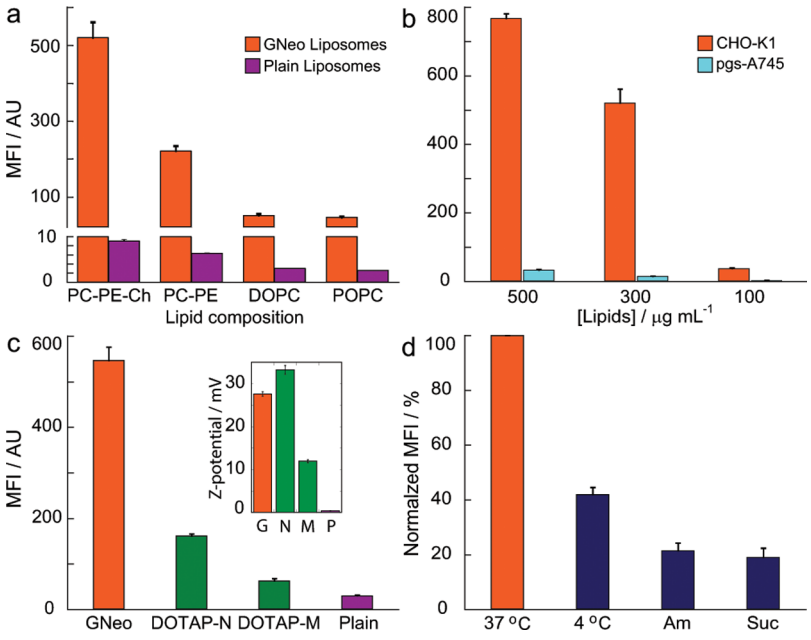

Figure 1. Cellular uptake. Cells were incubated with lipid vesicles for 1 h at 37 °C. Mean fluorescence intensity (MFI) was measured by flow cytometry. The background signal from untreated cells was subtracted. (a) Wild-type CHO-K1 cells incubated with plain and GNeo-decorated liposomes prepared with the indicated lipid composition. PC-PE-Ch = DOPC/DOPE/cholesterol, 73:11:16; PC-PE = DOPC/DOPE, 85:15. All GNeo-decorated liposomes contained 0.9 mol % stearyl-GNeo (4). (b) CHO-K1 cells and mutant pgsA-745 cells incubated with GNeosomes at the indicated concentrations. (c) CHO-K1 cells incubated with GNeosomes, lipid vesicles modified with DOTAP, and plain liposomes, all consisting of PC-PE-Chol, 73:11:16, at 300 μg mL^{-1}. DOTAP-M contains 0.9 mol % DOTAP and DOTAP-N contains 5.4 mol % DOTAP. Inset: Z-potential of the evaluated liposomes. G = GNeosomes, N = DOTAP-N, M = DOTAP-M, and P = plain liposomes. (d) CHO-K1 cells were incubated with GNeosomes (300 μg mL^{-1}) at 37 °C and at 4 °C. Cells were treated with amiloride (Am, 10 min, 5 mM) or sucrose (Suc, 1 h, 400 mM) at 37 °C prior to incubation with GNeosomes. The background signal from untreated cells was subtracted, and the MFI was normalized.

respectively). While introducing GNeo to the lipid vesicles increases the zeta potential only to 27 mV, flow cytometry revealed that GNeosomes display a 8.7- and 3.4-fold increase in cellular uptake when compared to DOTAP-M and DOTAP-N, respectively (Figure 1c).[28] These observations unequivocally demonstrate that the superior enhancement in cellular uptake imparted by GNeo is neither simply due to charge effect only nor a common feature of cationic liposomes. It highlights the importance of the 3D structure of guanidinoneomycin and the presentation of its guanidinium groups and supports the competent delivery capabilities and inherent affinity and selectivity of GNeosomes for cell surface glycosaminoglycans.

To better understand the internalization mechanism(s) of these previously unexplored lipid vesicles, the contribution of different endocytotic pathways was evaluated. Cellular uptake was therefore tested at low temperature (assessing the contribution of energy-dependent processes) and in cells pretreated with sucrose (impeding clathrin-mediated endocytosis) or with amiloride (hindering macropinocytosis). Interestingly, the internalization of GNeosomes and plain liposomes at low temperatures decreases to 40% and 60%, respectively (Figure 1d and Figure S6). Notably, in cells pretreated with sucrose, the internalization of plain liposomes was also lowered to 60%, while the entry of GNeosomes was reduced to 20% (Figure 1d and Figure S6). Furthermore, unlike the effect seen for GNeo−protein conjugates,[16] pretreating the cells with amiloride reduces the internalization of GNeo-based nanocarriers by 80%. This reduction in uptake was also observed for plain liposomes (Figure S6). Taken together, these results suggest that energy-dependent pathways are involved in the internalization of GNeosomes to a higher extent compared to plain liposomes. Background energy-independent binding and/or internalization take place, however, as uptake is also seen at low temperatures, as has been reported for certain liposomes and other carriers.[32−35]

Intracellular Localization. To elucidate the intracellular fate of these lipid vesicles, live cells were imaged by confocal laser scanning microscopy (CLSM) after 1 h incubation with carriers loaded with a water-soluble Cy5 dye and further treatment with the lysosomal marker LysoTracker Green DND-26 and the nuclear stain Hoechst 33342. Overlaying the images from the green and far red (pseudocolored in red) channels reveals a high degree of co-localization for GNeosomes and LysoTracker-stained compartments, while practically no co-localization is observed for plain liposomes, resulting in Pearson's correlation of 0.82 and 0.11, respectively (Figure 2). This observation suggests that decorating the liposomes with GNeo not only

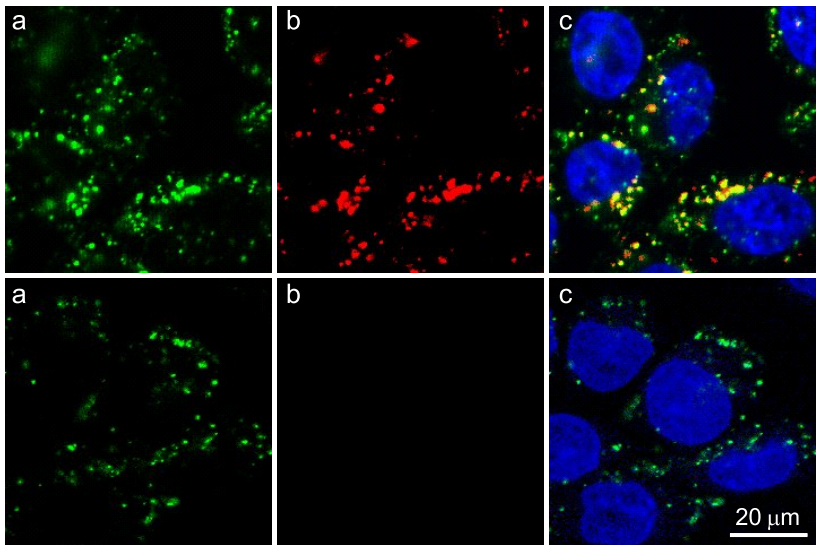

Figure 2. Intracellular localization of lipid vesicles. Upper panels: GNeosomes. Lower panels: Plain liposomes. (a) LysoTracker Green DND-26, (b) vesicles loaded with Cy5, and (c) merged images with nuclear Hoechst dye. See Figure S7 for larger field images.

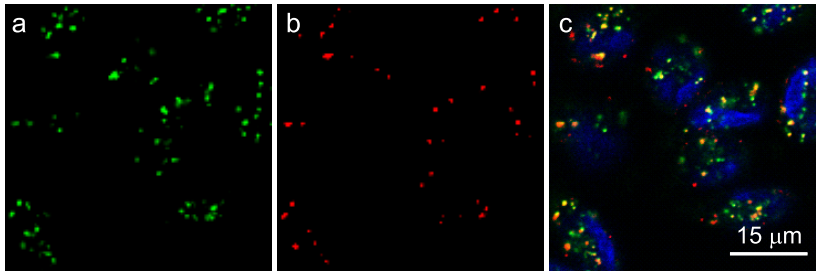

Figure 3. Cellular uptake of GNeosomes loaded with streptavidin-Cy3. (a) LysoTracker Green DND-26, (b) GNeosomes, and (c) merged images with Hoechst dye.

drastically enhances their cellular uptake but, most importantly, selectively directs them to the target organelle.

Delivery of Biomacromolecules. To investigate the cellular delivery of high molecular weight proteins, GNeosomes were loaded with a fluorescently labeled streptavidin (ST-Cy3; 60 kDa). Cells were incubated with GNeosomes for 1 h and further treated with the lysosomal marker LysoTracker Green DND-26 and the nuclear stain Hoechst 33342. Overlaying the images from the green and red channels reveals a high degree of co-localization for GNeosomes and LysoTracker-stained organelles (Figure 3). Moreover, flow cytometry analysis comparing the cellular delivery of ST-Cy3 loaded either in plain liposomes or in GNeosomes shows a high increase in the MFI for the cells treated with the latter (Figure S8). Importantly, live cell imaging together with flow cytometry analysis unambiguously demonstrates the ability of GNeosomes to efficiently deliver these biomacromolecules to the lysosomes.

Lysosomal Release of Cargo. While cellular internalization is obviously a key step, intracellular trafficking and release are critical for any fundamental cellular investigation or therapeutic application. To confirm that the cargo loaded in GNeosomes is released in the lysosomes, LysoSensor Dextran Blue/Yellow (MW = 10.000) was used. The readout of this intracellular pH indicator is based on a ratiometric analysis between the fluorescent intensity of "green" and "blue" emission bands, which increases as pH decreases.[36] CHO-K1 cells were incubated either with GNeosomes loaded with LysoSensor or with nonencapsulated LysoSensor, and live cells were imaged by CLSM using LysoTracker Deep Red to mark the lysosomes. Overlaying the LysoTracker signal with either the "blue" or "green" channels clearly shows higher lysosomal co-localization for GNeosomes compared to the nonencapsulated LysoSensor (Figure 4a,b and Figure S9). Furthermore, the areas in which co-localization is more evident (*i.e.*, yellow puncta in Figure 4a and b, white arrows) show the highest intensity in the ratiometric images (Figure 4c and d, red arrows). This correlation strongly suggests that the cargo, originally encapsulated in GNeosomes at pH 7.4, was released into a more acidic environment resembling that surrounding the nonencapsulated LysoSensor and is thus found free in the lysosomes.

To further quantify the increase in lysosomotropism of GNeosomes compared to plain liposomes, these

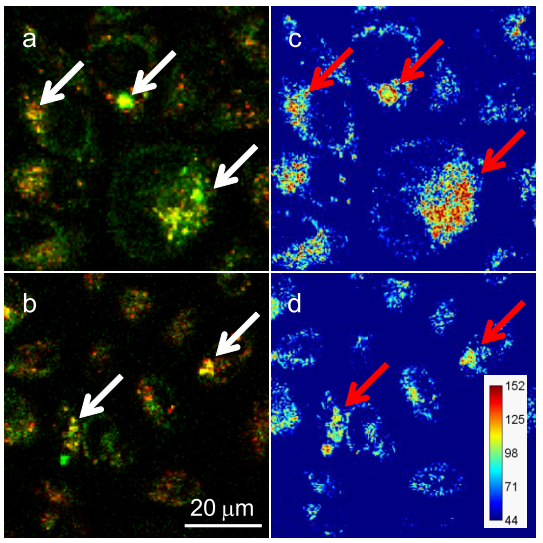

Figure 4. Release of cargo in the lysosomes. Upper panels: GNeosomes loaded with LysoSensor. Lower panels: Nonencapsulated LysoSensor. (a and b) Merged images showing the "green" channel and LysoTracker Deep Red (pseudocolored in red). (c and d) Ratiometric images showing the ratio between the fluorescent intensity of the "green" and "blue" channels.

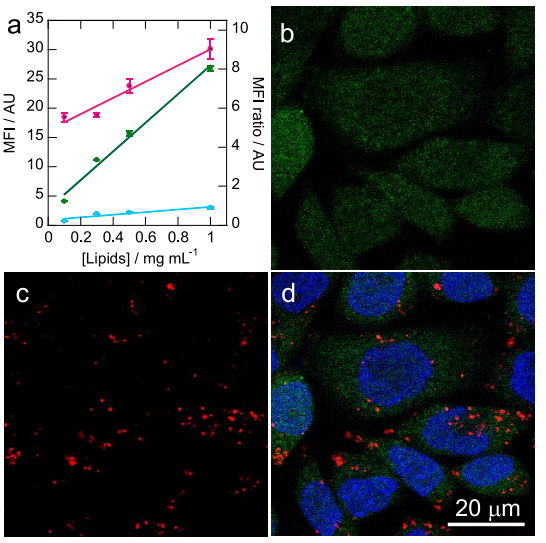

Figure 5. Lysosomal delivery of FDG. (a) Flow cytometry of lysosomal targeting by liposomes loaded with FDG. CHO-K1 cells were incubated for 1 h with GNeosomes (green) or plain liposomes (cyan) at the indicated concentrations. The background signal from untreated cells was subtracted, and the ratio between the signals from GNeosomes and plain liposomes was calculated (magenta). (b, c, and d) CLSM images of CHO-K1 cells incubated for 1 h with GNeosomes loaded with FDG: (b) fluorescein, released from FDG shown in green, (c) LysoTracker Deep Red (pseudocolored in red), and (d) an overlay of b and c including the nuclear stain Hoechst.

lipid vesicles were loaded with fluorescein di-β-D-galactopyranoside (FDG), a fluorogenic substrate for the intralysosomal enzyme β-galactosidase (β-Gal). Upon hydrolysis by β-Gal in the lysosome, the released fluorescein can be quantified by FACS and visualized by CLSM. Incubating wild-type cells with either GNeo-decorated or plain liposomes and further quantification of the lysosomal delivery demonstrates that GNeosomes are remarkably more lysosomotropic than plain liposomes, as the ratio between the MFI observed for GNeosomes and that for plain liposomes shows up to 9-fold enhancement under these experimental conditions (Figure 5a, Table S2). The dose-dependent increase in the signal arising from the enzymatic activity of β-Gal implies that the lysosomal presence of GNeosomes, intact or degraded, does not inhibit the enzyme. Interestingly, live cell imaging of wild-type CHO-K1 treated with GNeosomes encapsulating FDG reveals diffuse green fluorescence, consistent with fluorescein's lysosomal escape, as reported by Straubinger *et al.* (Figure 5b).[37] Furthermore, as observed in Figures 2–4, the punctated appearance of the lysosomes is not disrupted, suggesting that their integrity is maintained (Figure 5c and d). These observations are in agreement with the high degree of lysosomal co-localization displayed by GNeosomes, reinforcing the notion of GNeo-enhanced lysosomotropism.

Lipid vesicles as nanocarriers for bioactive cargo have significantly advanced in recent years, and several liposome-based drugs have been approved by the FDA.[38,39] Liposomes decorated with cell-penetrating peptides such as HIV-1 Tat, antennapedia, and $(Arg)_8$ have been reported to facilitate cellular uptake of different cargos, which were found mainly in the cytoplasm and to lesser extents in the nucleus.[40–43] Linking targeting moieties to lipid vesicles proved useful for their delivery to well-defined intracellular compartments such as the mitochondria, ER, and lysosomes.[44–49] Attempts to increase the lysosomal affinity of lipid vesicles by decorating them with either high molecular weight proteins (*e.g.*, transferrin 80 kDa) or low MW ligands (*e.g.*, rhodamine B) resulted, however, in a relatively low increase in lysosomotropism (less than 2-fold), urging the need for the development of more selective and efficient targeting devices.[13,45,47,48] GNeosomes thus show not only dramatically enhanced cellular uptake compared to liposomes but an unprecedented high increase in lysosomotropism, illustrating that GNeo serves two key functions, yielding highly efficient lysosome-targeting cellular nanocarriers.

CONCLUSIONS

In summary, we have developed a new highly specific lysosomotropic nanocarrier platform based on lipid vesicles decorated with guanidinoneomycin, termed GNeosomes. Through their high affinity for cell surface glycosaminoglycans, GNeosomes are able to enter the cells and subsequently deliver a variety of cargo, ranging from small molecules to large biomacromolecules, to the lysosomes. The increased interest in lysosomal malfunction, once thought to be associated only with genetic lysosomal storage disorders,

suggests that targeted delivery to the lysosome is likely to find utility as a research tool and as a vehicle for therapeutic delivery. As new observations are made associating complex cellular pathways (such as apoptosis) and multifaceted neurological diseases (such as Parkinson's disease) with lysosomal failure,[3,4] a universal lysosomal delivery system, such as GNeosomes, may become of key utility.

EXPERIMENTAL SECTION

Stearyl-GNeo was synthesized according to detailed synthetic procedures presented in Supporting Information Scheme S1.

Preparation of GNeo-Containing Liposomes. A mixture (15 mg total) of DOPC (1,2-dioleoyl-*sn*-glycero-3-phosphocholine), DOPE (1,2-dioleoyl-*sn*-glycero-3-phosphoethanolamine), and cholesterol (73:11:16) was dissolved in chloroform to a final volume of 1 mL and evaporated in a round flask to form a thin lipid layer. Any solvent remaining was removed under high vacuum overnight. The resulting film was hydrated for 10 min at 40 °C with 1 mL of PBS containing Stearyl-GNeo (0.36 mg, 0.9 mol %) and the cargo (any of the following: a water-soluble cyanine dye prepared as reported,[29] 100 μM; streptavidin-Cy3, 0.6 mg mL^{-1}; LysoSensor Dextran Yellow/Blue, 1 mg mL^{-1}; fluorescein di-β-D-galactopyranoside, 200 μM). The mixture was sonicated for 30 s to completely detach the lipids, forming a fine suspension, and subjected to six freeze/thaw cycles using a dry ice/acetone bath (1 min) and a water bath at 40 °C (1.5 min). Finally the suspension was extruded 17 times through a polycarbonate membrane (pore size 100 nm) at room temperature. Extravesicular components were removed by gravitational gel filtration (Sephadex G-50 for small molecules or Sepharose 4B for dextran and streptavidin derivatives), eluting with PBS. The desired size distribution was verified by dynamic light scattering analysis, and lipid concentration was determined adapting the Stewart method.[50]

Preparation of Liposomes. Plain liposomes were prepared as described above without adding stearyl-GNeo.

Determination of Lipids in Liposomal Suspensions. After purification by size exclusion, lipid concentration was determined adapting the Stewart method.[50] Briefly, an aliquot of the liposomal suspension was diluted to an approximate lipid concentration of 0.25 mg/mL. To 2.5 mL of chloroform was added 100 μL of the diluted liposomes followed by 2.5 mL of ammonium ferrothiocyanate (0.1 M). The biphasic system was vigorously vortexed for 20 s and further centrifuged for 1 min. The optical density of the organic phase was measured at 480 nm against chloroform as a blank. The amount of lipids present was estimated by comparison to a calibration curve generated using liposomal suspensions with a known lipid content.

Cell Culture. All cells were grown under an atmosphere of 5% CO_2 in air and 100% relative humidity. Wild-type Chinese hamster ovary cells (CHO-K1) were obtained from the American Type Culture Collection (CCL-61), and pgsA-745 cells were prepared as previously reported.[31,51] CHO-K1 and pgsA-745 cells were grown in F-12 medium (Life Technologies) supplemented with fetal bovine serum (10% v/v), streptomycin sulfate (100 μg/mL), and penicillin G (100 units/mL). The Hep3B cell line was obtained from ATCC (HB-8064) and cultured in MEM (Invitrogen) supplemented with 10% fetal bovine serum (Gemini Bio-Products), nonessential amino acids, penicillin (100 units/mL), and streptomycin (100 μg/mL). HEK293T cells were obtained from ATCC and maintained in Dulbecco's modified Eagle medium (DMEM) supplemented with 10% FBS, penicillin (100 units/mL), and streptomycin (100 μg/mL).

Encapsulation Efficiency. EE was calculated as the ratio between the fluorescence intensity (640/672) of 1 mL of a methanolic solution of lipid vesicles (0.1 mg/mL) before and after size exclusion purification. See Figure S2.

Cell Viability. CHO-K1 cells were seeded in a 96-well plate at a density of 20 000 cells per well. After growing overnight, the cells were treated with liposomes and GNeosomes at the indicated concentrations in serum-free medium and incubated for 24 h. Cells were washed, and the growth medium was replaced. Cell Titer Blue (20 μL) was added to each well, and the cells were incubated for 4 h at 37 °C. Fluorescence was measured in a plate reader with excitation/emission wavelengths set at 530/580. Fluorescence intensity was normalized to that of untreated cells.

Cellular Uptake. Wild-type CHO-K1, HEK293T, Hep3B, and mutant pgsA cells were seeded onto 24-well tissue culture plates (100 000 cells/well, 0.5 mL; 250 000 cells/well for Hep3B) and grown for 24 h to about 80% confluence. Cells were washed with PBS and incubated with 300 μL of the liposomal suspension diluted in growth medium containing 10% FBS to the desired concentration and incubated at 37 °C for 1 h under an atmosphere of 5% CO_2. The cells were washed twice with 300 μL of PBS twice, detached with 100 μL of trypsin-EDTA (Life Technologies) at 37 °C for 5 min, diluted with PBS containing 1% BSA, and analyzed by FACS.

Evaluation of Clathrin-Dependent Endocytosis and Macropinocytosis of Liposomes. Cells were grown for 24 h as described above, washed with PBS, and incubated with 400 mM sucrose or 5 mM amiloride for 1 h or 10 min, respectively. Cells were then washed with PBS and treated with 300 μL of the liposomal suspension diluted in growth medium to 300 μg/mL and incubated at 37 °C for 1 h under an atmosphere of 5% CO_2. Cells were washed with PBS, detached with trypsin-EDTA, and analyzed as described above.

Evaluation of Uptake Dependency on Temperature. Cells were grown for 24 h as described above, washed with PBS, and incubated for 30 min at 4 °C in F-12. Precooled liposomes, diluted in F-12 to 300 μg/mL, were added to the cooled cells and incubated for 30 min at 4 °C. Cells were washed, detached, and analyzed as described above.

Fluorescence Microscopy. CHO-K1 cells were grown for 24 h in 35 mm dishes equipped with a glass bottom coverslip coated with poly-D-lysine. Cells were washed with PBS, treated with 1.5 mL of liposomal suspension diluted in growth medium to 1 mg/mL, and incubated at 37 °C for 1 h under an atmosphere of 5% CO_2. Cells were then washed with PBS, stained with the appropriate dye (Hoechst, LysoTracker), and kept in DMEM phenol red-free medium for imaging.

Ratiometric Analysis. Cells were grown in 35 mm dishes as above and incubated with 1.5 mL of LysoSensor Dextran Blue/Yellow or with GNeosomes (encapsulating LysoSensor Dextran Blue/Yellow) diluted in growth medium to 1 mg/mL at 37 °C for 1 h under an atmosphere of 5% CO_2. Cells were then washed with PBS and kept in DMEM phenol red-free medium for imaging. Both "blue" and "green" exciting lasers were set at 405 nm. Images were processed and analyzed using Nikon Imaging Software Elements and ImageJ (NIH).

Conflict of Interest: The authors declare no competing financial interest.

Supporting Information Available: Materials, instrumentation and synthetic procedures, NMR spectra, and supporting figures are supplied as Supporting Information. This material is available free of charge *via* the Internet at http://pubs.acs.org.

Acknowledgment. We thank the National Institutes of Health (GM077471 to Y.T. and J.D.E.), National Science Foundation (CHE-1303554 to Y.T.), and the W. M. Keck Foundation (Y.T.) for support. This work was also supported in part by a research grant from the University of Pennsylvania Center for Orphan Disease Research and Therapy (J.D.E). Confocal microscopy imaging was supported by the UCSD Specialized Cancer Center Support Grant P30 2P30CA023100-28 from NCI. We thank A. Fin (Chemistry and Biochemistry, UCSD) for technical help and useful discussions, W. Tong (Cellular Molecular Medicine, UCSD) for help with cell culture, Y. Su (Mass Spectrometry Facility,

Chemistry and Biochemistry, UCSD) for help with sample analysis, and the Gianneschi lab (Chemistry and Biochemistry, UCSD) for the use of their light scattering device. We also thank the Zhang lab (Nanoengineering, UCSD) for the use of their Zetasizer to measure zeta potentials.

REFERENCES AND NOTES

1. Luzio, J. P.; Pryor, P. R.; Bright, N. A. Lysosomes: Fusion and Function. *Nat. Rev. Mol. Cell. Biol.* **2007**, *8*, 622–632.
2. Winchester, B.; Vellodi, A.; Young, E. The Molecular Basis of Lysosomal Storage Diseases and their Treatment. *Biochem. Soc. Trans.* **2000**, *28*, 150–154.
3. Sidransky, E.; Lopez, G. The Link between the GBA Gene and Parkinsonism. *Lancet Neurol.* **2012**, *11*, 986–998.
4. Westbroek, W.; A. Gustafson, M.; Sidransky, E. Exploring the Link between Glucocerebrosidase Mutations and Parkinsonism. *Trends Mol. Med.* **2011**, *17*, 485–493.
5. Appelqvist, H.; Wäster, P.; Kågedal, K.; Öllinger, K. The Lysosome: From Waste Bag to Potential Therapeutic Target. *J. Mol. Cell Biol.* **2013**, *5*, 214–226.
6. Rin Jean, S.; Tulumello, D. V.; Wisnovsky, S. P.; Lei, E. K.; Pereira, M. P.; Kelley, S. O. Molecular Vehicles for Mitochondrial Chemical Biology and Drug Delivery. *ACS Chem. Biol.* **2014**, *9*, 323–333.
7. Torchilin, V. P. Recent Approaches to Intracellular Delivery of Drugs and DNA and Organelle Targeting. *Annu. Rev. Biomed. Eng.* **2006**, *8*, 343–375.
8. Giannotti, M. I.; Esteban, O.; Oliva, M.; Garcia-Parajo, M. F.; Sanz, F. pH-Responsive Polysaccharide-Based Polyelectrolyte Complexes as Nanocarriers for Lysosomal Delivery of Therapeutic Proteins. *Biomacromolecules* **2011**, *12*, 2524–2533.
9. Maniganda, S.; Sankar, V.; Nair, J. B.; Raghu, K. G.; Maiti, K. K. A Lysosome-Targeted Drug Delivery System Based on Sorbitol Backbone towards Efficient Cancer Therapy. *Org. Biomol. Chem.* **2014**, *12*, 6564–6569.
10. Oh, N. M.; Oh, K. T.; Youn, Y. S.; Lee, D.-K.; Cha, K.-H.; Lee, D. H.; Lee, E. S. Poly(L-aspartic acid) Nanogels for Lysosome-Selective Antitumor Drug Delivery. *Colloids Surf., B* **2013**, *101*, 298–306.
11. Zhu, S.; Lansakara-P, D. S. P.; Li, X.; Cui, Z. Lysosomal Delivery of a Lipophilic Gemcitabine Prodrug Using Novel Acid-Sensitive Micelles Improved Its Antitumor Activity. *Bioconjugate Chem.* **2012**, *23*, 966–980.
12. Nair, J. B.; Mohapatra, S.; Ghosh, S.; Maiti, K. K. Novel Lysosome Targeted Molecular Transporter Built on a Guanidinium-poly-(propylene imine) Hybrid Dendron for Efficient Delivery of Doxorubicin into Cancer Cells. *Chem. Commun.* **2015**, *51*, 2403–2406.
13. Meerovich, I.; Koshkaryev, A.; Thekkedath, R.; Torchilin, V. P. Screening and Optimization of Ligand Conjugates for Lysosomal Targeting. *Bioconjugate Chem.* **2011**, *22*, 2271–2282.
14. Baker, T. J.; Luedtke, N. W.; Tor, Y.; Goodman, M. Synthesis and Anti-HIV Activity of Guanidinoglycosides. *J. Org. Chem.* **2000**, *65*, 9054–9058.
15. Luedtke, N. W.; Carmichael, P.; Tor, Y. Cellular Uptake of Aminoglycosides, Guanidinoglycosides, and Poly-Arginine. *J. Am. Chem. Soc.* **2003**, *125*, 12374–12375.
16. Elson-Schwab, L.; Garner, O. B.; Schuksz, M.; Crawford, B. E.; Esko, J. D.; Tor, Y. Guanidinylated Neomycin Delivers Large, Bioactive Cargo into Cells through a Heparan Sulfate-Dependent Pathway. *J. Biol. Chem.* **2007**, *282*, 13585–13591.
17. Bishop, J. R.; Schuksz, M.; Esko, J. D. Heparan Sulphate Proteoglycans Fine-Tune Mammalian Physiology. *Nature* **2007**, *446*, 1030–1037.
18. Xu, D.; Esko, J. D. Demystifying Heparan Sulfate−Protein Interactions. *Annu. Rev. Biochem.* **2014**, *83*, 129–157.
19. Sarrazin, S.; Wilson, B.; Sly, W. S.; Tor, Y.; Esko, J. D. Guanidinylated Neomycin Mediates Heparan Sulfate-Dependent Transport of Active Enzymes to Lysosomes. *Mol. Ther.* **2010**, *18*, 1268–1274.
20. Dix, A. V.; Fischer, L.; Sarrazin, S.; Redgate, C. P.; Esko, J. D.; Tor, Y. Cooperative, Heparan Sulfate-Dependent Cellular Uptake of Dimeric Guanidinoglycosides. *ChemBioChem* **2010**, *11*, 2302–2310.
21. Inoue, M.; Tong, W.; Esko, J. D.; Tor, Y. Aggregation-Mediated Macromolecular Uptake by a Molecular Transporter. *ACS Chem. Biol.* **2013**, *8*, 1383–1388.
22. Natarajan, A.; Du, W.; Xiong, C. Y.; DeNardo, G. L.; DeNardo, S. J.; Gervay-Hague, J. Construction of di-scFv through a Trivalent Alkyne-Azide 1,3-Dipolar Cycloaddition. *Chem. Commun.* **2007**, *7*, 695–697.
23. Related derivatives were reported. See refs 24−27.
24. Sainlos, M.; Belmont, P.; Vigneron, J.-P.; Lehn, P.; Lehn, J.-M. Aminoglycoside-Derived Cationic Lipids for Gene Transfection: Synthesis of Kanamycin A Derivatives. *Eur. J. Org. Chem.* **2003**, *15*, 2764–2774.
25. Sainlos, M.; Hauchecorne, M.; Oudrhiri, N.; Zertal-Zidani, S.; Aissaoui, A.; Vigneron, J.-P.; Lehn, J.-M.; Lehn, P. Kanamycin A-Derived Cationic Lipids as Vectors for Gene Transfection. *ChemBioChem* **2005**, *6*, 1023–1033.
26. Mével, M.; Sainlos, M.; Chatin, B.; Oudrhiri, N.; Hauchecorne, M.; Lambert, O.; Vigneron, J.-P.; Lehn, P.; Pitard, B.; Lehn, J.-M. Paromomycin and Neomycin B Derived Cationic Lipids: Synthesis and Transfection Studies. *J. Controlled Release* **2012**, *158*, 461–469.
27. Bera, S.; Dhondikubeer, R.; Findlay, B.; Zhanel, G. G.; Schweizer, F. Synthesis and Antibacterial Activities of Amphiphilic Neomycin B-Based Bilipid Conjugates and Fluorinated Neomycin B-Based Lipids. *Molecules* **2012**, *17*, 9129–9141.
28. Encapsulation efficiency remains unaffected by the addition of **4** (Figure S2).
29. Kojima, R.; Takakura, H.; Ozawa, T.; Tada, Y.; Nagano, T.; Urano, Y. Rational Design and Development of Near-Infrared-Emitting Firefly Luciferins Available *in Vivo*. *Angew. Chem., Int. Ed.* **2013**, *52*, 1175–1179.
30. Our observations are not limited to CHO cells. Substantially enhanced uptake was also seen in HEK293T and Hep3B cell lines. See Figure S3.
31. Esko, J. D.; Stewart, T. E.; Taylor, W. H. Animal-Cell Mutants Defective in Glycosaminoglycan Biosynthesis. *Proc. Natl. Acad. Sci. U.S.A.* **1985**, *82*, 3197–3201.
32. Gasparini, G.; Bang, E.-K.; Molinard, G.; Tulumello, D. V.; Ward, S.; Kelley, S. O.; Roux, A.; Sakai, N.; Matile, S. Cellular Uptake of Substrate-Initiated Cell-Penetrating Poly(disulfide)s. *J. Am. Chem. Soc.* **2014**, *136*, 6069–6074.
33. Iwasa, A.; Akita, H.; Khalil, I.; Kogure, K.; Futaki, S.; Harashima, H. Cellular Uptake and Subsequent Intracellular Trafficking of R8-Liposomes Introduced at Low Temperature. *BBA-Biomembranes* **2006**, *1758*, 713–720.
34. Mitchell, D. J.; Steinman, L.; Kim, D. T.; Fathman, C. G.; Rothbard, J. B. Polyarginine Enters Cells More Efficiently than Other Polycationic Homopolymers. *J. Pept. Res.* **2000**, *56*, 318–325.
35. Torchilin, V. P.; Rammohan, R.; Weissig, V.; Levchenko, T. S. TAT Peptide on the Surface of Liposomes Affords Their Efficient Intracellular Delivery Even at Low Temperature and in the Presence of Metabolic Inhibitors. *Proc. Natl. Acad. Sci. U.S.A.* **2001**, *98*, 8786–8791.
36. Diwu, Z. J.; Chen, C. S.; Zhang, C. L.; Klaubert, D. H.; Haugland, R. P. A Novel Acidotropic pH Indicator and Its Potential Application in Labeling Acidic Organelles of Live Cells. *Chem. Biol.* **1999**, *6*, 411–418.
37. Straubinger, R. M.; Hong, K.; Friend, D. S.; Papahadjopoulos, D. Endocytosis of Liposomes and Intracellular Fate of Encapsulated Molecules - Encounter with a Low pH Compartment after Internalization in Coated Vesicles. *Cell* **1983**, *32*, 1069–1079.
38. Chang, H. I.; Yeh, M. K. Clinical Development of Liposome-Based Drugs: Formulation, Characterization, and Therapeutic Efficacy. *Int. J. Nanomed.* **2012**, *7*, 49–60.
39. Slingerland, M.; Guchelaar, H. J.; Gelderblom, H. Liposomal Drug Formulations in Cancer Therapy: 15 Years along the Road. *Drug Discovery Today* **2012**, *17*, 160–166.
40. Torchilin, V. P. Cell Penetrating Peptide-Modified Pharmaceutical Nanocarriers for Intracellular Drug and Gene Delivery. *J. Pept. Sci.* **2008**, *90*, 604–610.

41. Cryan, S.-A.; Devocelle, M.; Moran, P. J.; Hickey, A. J.; Kelly, J. G. Increased Intracellular Targeting to Airway Cells Using Octaarginine-Coated Liposomes: *In Vitro* Assessment of Their Suitability for Inhalation. *Mol. Pharmaceutics* **2006**, *3*, 104–112.
42. Console, S.; Marty, C.; Garcia-Echeverria, C.; Schwendener, R.; Ballmer-Hofer, K. Antennapedia and HIV Transactivator of Transcription (TAT) "Protein Transduction Domains" Promote Endocytosis of High Molecular Weight Cargo upon Binding to Cell Surface Glycosaminoglycans. *J. Biol. Chem.* **2003**, *278*, 35109–35114.
43. Marty, C.; Meylana, C.; Schottb, H.; Ballmer-Hofer, K.; Schwendener, R. A. Enhanced Heparan Sulfate Proteoglycan-Mediated Uptake of Cell-Penetrating Peptide-Modified Liposomes. *Cell. Mol. Life Sci.* **2004**, *61*, 1785–1794.
44. Biswas, S.; Dodwadkar, N. S.; Deshpande, P. P.; Torchilin, V. P. Liposomes Loaded with Paclitaxel and Modified with Novel Triphenylphosphonium-PEG-PE Conjugate Possess Low Toxicity, Target Mitochondria and Demonstrate Enhanced Antitumor Effects *in Vitro* and *in Vivo*. *J. Controlled Release* **2012**, *159*, 393–402.
45. Koshkaryev, A.; Thekkedath, R.; Pagano, C.; Meerovich, I.; Torchilin, V. P. Targeting of Lysosomes by Liposomes Modified with Octadecyl-Rhodamine B. *J. Drug Target* **2011**, *19*, 606–614.
46. Pollock, S.; Antrobus, R.; Newton, L.; Kampa, B.; Rossa, J.; Latham, S.; Nichita, N. B.; Dwek, R. A.; Zitzmann, N. Uptake and Trafficking of Liposomes to the Endoplasmic Reticulum. *FASEB J.* **2010**, *24*, 1866–1878.
47. Koshkaryev, A.; Piroyan, A.; Torchilin, V. P. Increased Apoptosis in Cancer Cells *in Vitro* and *in Vivo* by Ceramides in Transferrin-Modified Liposomes. *Cancer Biol. Ther.* **2012**, *13*, 50–59.
48. Thekkedath, R.; Koshkaryev, A.; Torchilin, V. P. Lysosome-Targeted Octadecyl-Rhodamine B-Liposomes Enhance Lysosomal Accumulation of Glucocerebrosidase in Gaucher's Cells *in Vitro*. *Nanomedicine* **2013**, *8*, 1055–1065.
49. Muro, S.; Schuchman, E. H.; Muzykantov, V. R. Lysosomal Enzyme Delivery by ICAM-1-Targeted Nanocarriers Bypassing Glycosylation- and Clathrin-Dependent Endocytosis. *Mol. Ther.* **2006**, *13*, 135–141.
50. Stewart, J. C. M. Colorimetric Determination of Phospholipids with Ammonium Ferrothiocyanate. *Anal. Biochem.* **1980**, *104*, 10–14.
51. Bai, X. M.; Wei, G.; Sinha, A.; Esko, J. D. Chinese Hamster Ovary Cell Mutants Defective in Glycosaminoglycan Assembly and Glucuronosyltransferase I. *J. Biol. Chem.* **1999**, *274*, 13017–13024.